British Journal of Pharmaceutical Research
4(1): 37-59, 2014

SCIENCEDOMAIN *international*
www.sciencedomain.org

Optimized Artemether-loaded Anhydrous Emulsion

N. C. Obitte[1], L. C. Rohan[2*], C. M. Adeyeye[3] and C. O. Esimone[4]

[1]Department of Pharmaceutical Technology and Industrial Pharmacy, Faculty of Pharmaceutical Sciences, University of Nigeria, Nsukka, Nigeria.
[2]Department of Pharmaceutical Sciences, School of Pharmacy, Magee Womens Research Institute, University of Pittsburgh, Pittsburgh, PA, USA.
[3]Department of Biopharmaceutical Sciences, College of Pharmacy, Roosevelt University Schaumburg, IL, USA.
[4]Department of Pharmaceutical Microbiology and Biotechnology, Faculty of Pharmaceutical Sciences, Nnamdi Azikiwe University, Awka, Anambra State, Nigeria.

Authors' contributions

This work was carried out in collaboration between all authors. All the authors were involved in the conception, design and execution of the work. Author NCO performed the statistical analysis, wrote the protocol, and wrote the first draft of the manuscript. All authors were involved in the proofreading and approval of the final manuscript.

Research Article

Received 12th June 2013
Accepted 31st July 2013
Published 5th October 2013

ABSTRACT

Objective: The objectives of this study were to identify stable anhydrous emulsions via pseudo ternary phase diagram, optimize artemether-loaded batches using factorial design and subsequently evaluate the antimalarial activity.
Methodology: Using labrasol®, triacetin® and lauroglycol 90® as the surfactant, oil and co-surfactant respectively, pseudo ternary phase diagram was generated from the quantitative titration of water with the anhydrous emulsion. Stable combinations from the phase diagram were subjected to a 2^3 full factorial experimental design. The 22 software-generated formulations were experimentally formulated and characterized for droplet size, polydispersity index, viscosity and thermodynamic stability. Droplet size was chosen and subsequently fitted into the Response column of the software, thus prompting the generation of graphs and Desirability table of 125 predicted formulations. Out of the 125 predictions, three with the least droplet sizes (less than 100 nm) were adjudged as

**Corresponding author: Email: lrohan@mwri.magee.edu;*

optimized batches. Subsequently, they were formulated, converted to powder by adsorption on magnesium aluminum metasilicate and evaluated. Antimalarial effectiveness of the drug-loaded formulation was also investigated.
Results: Triacetin® most significantly (P<0.05) contributed to droplet size variation. The droplet size of the experimental formulations approximated that of the statistical predictions. The anhydrous emulsions (AEs) were powderable and the granulations rated fair and passable according to Carr's scale. Artemether-loaded anhydrous emulsion (AE) demonstrated highest antimalarial activity.
Conclusion: We therefore conclude that optimization proved a useful tool for the identification of excipient proportions with optimal effects.

Keywords: Anhydrous emulsion; optimized; pseudoternary phase diagram; droplet size; Flow properties; antimalarial activity.

1. INTRODUCTION

Self-emulsifying oil formulation (SEF) is a technical acronym for self-emulsifying drug delivery system (SEDDS), self-nano-emulsifying drug delivery system (SNEDDS) and self-micro-emulsifying drug delivery system (SMEDDS). SMEDDS and SNEDDS form micro-emulsions and nano-emulsions respectively in aqueous phase with droplet sizes of less than or equal to 100 nm while SEDDS are emulsions with droplet sizes of above 100 nm. SNEDDS are kinetically stable while SMEDDS are thermodynamically stable. SEF is an approach that addresses the poor water solubility characteristic of a good number of active pharmaceutical ingredients. The concept and development of micro-emulsion was pioneered by Schulman (and his fellow workers) reputed to have initiated the name microemulsion [1,2]. SEFs are isotropic, anhydrous mixtures of oil, surfactant and cosurfactant which on gentle agitation in aqueous medium undergo self-emulsification to yield oil-in-water emulsions or micro-emulsions [3,4].

SEF is credited with the following functional and mechanistic advantages, including provision of a milieu for the improvement of the solubility of poorly soluble drugs; ease of autoclaving; opening of tight junction for paracellular transport; facilitation of membrane fluidity for the promotion of transcellular absorption; inhibition of the efflux transporter P-gp and improvement on bioavailability [5]. Lymphatic absorption and transport can be achieved through transcellular pathway or promotion of lipoprotein synthesis by enterocytes and lipids including SEFs [6-10].

The artemisinin group of antimalarials was thought to be the therapeutic solution to malaria pandemic amongst African blacks. However, it was discovered that the drawback suffered by chloroquine, that is resistance and compromised potency, was also potentially possible with the artemisinin group, hence the resort to the popular artemisinin combination therapy (ACT) with other antimalaria drugs. Artemether is a poorly soluble derivative of artemisinin, that may be associated with inconsistent bioavailability when orally ingested. Inconsistent absorption may create sublethal systemic and tissue drug levels with potential for inducing drug resistance. Thus the prescription instruction to co-administer with fatty meal was believed to improve gastro intestinal tract solubility, absorption and systemic bioavailability [11,12]. However information on the fraction of fat in food or optimal quantity of needed fat is often not part of the drug product information. The co-administration with fatty meal may, precariously predispose to drug-food interaction capable of defeating the bioavailability

enhancement goal. Therefore a lipid-based formulation carrier that will have artemether intact as soluble drug will culminate in invents that may maintain lumen solubility and enhanced consistent absorption profile. This is what SEF is proposed to achieve in this study. The presence of surfactants in this formulation approach may additionally provide a permeability-enhancement effect in the gut lumen.

Commercial availability of Neoral® (cyclosporine A), Norvir® (ritonavir), Fortavase® (saquinavir) and Aptivus® (tipranavir) SEDDS [13, 14] portend future industrial and commercial prospects for SEF technology. Apart from patent cost and restrictions, blazing the trail in industrializing novel findings seem to require much gut. Manufacturers may be wooed if such incentives as, low or moderate production costs and practicability/reproducibility of formulation processes (validation) are guaranteed. To help industrialists answer their economic questions scientists introduced optimization approach to ascertain the minimum formulation constituents required to maximize therapeutic efficacy and by extrapolation, profit. Hence the adoption of statistical methods to, optimize formulation constituents and save scientific resources [15]. Several applications of factorial experimental design and response surface methodology in optimization of formulation constituents [16-19] have been documented.

The presence and multiple effects of two or more excipients involved in SEF formulations impel the application of optimization methods to determine their optimal quantitative contributions on self-emulsification and other parameters. Typically the traditional approach which involves the application of pseudo ternary phase diagram has been the preference of many workers [12,20,21]. However, some workers [22] used 3^2 factorial design (incorporating response surface methodology and multiple regressions) to study the effect of concentrations of cosurfactant and gelling agent on emulsification process and drug diffusion. Their study did not involve a preliminary pseudo ternary phase diagram construction. Similarly, central composite experimental design was used to optimize amisulpride self-emulsifying drug delivery system, without pseudo ternary phase diagram *ab initio* [23]. Response surface methodology has also been used to optimize celecoxib via 3^3 design format, without initial resort to pseudo ternary phase diagram construction [24]. Pseudo ternary phase diagram is a type of optimization technique preliminarily conducted as preformulation unit operation. It creates boundary-map information on the type of dispersions formed with different constituent proportions [25]. By delineating self-emulsifying regions, poor and good emulsion compositions may be identified. Self-emulsification (with optical clarity), one of several characteristics of SEFs, is the prominent response considered. We therefore thought that the employment of a follow-up experimental design might provide a more flexible platform for optimization, incorporating several other parameters or responses at a time. For instance viscosity, droplet size, release profile, etc can be considered simultaneously. This will be of industrial significance to manufacturers of artemether in malaria-infested regions of the world, as per cost and availability. The employment of factorial design may result to cost-effectiveness since the minimum but optimally effective concentrations are predictable. In our present investigation we are proposing that in addition to pseudo ternary phase diagram, further optimization approach will be an attractive and robust initiative to manufacturers. Hence the objectives of this study were, to identify stable anhydrous emulsions (AEs) through pseudo ternary phase diagram construction, formulate optimized artemether-loaded batches using, 2^3 full, factorial experimental design, transform them into powder and carry out some *in vitro* and antimalarial studies.

2. MATERIALS AND METHODS

2.1 Materials

Triacetin (Acros Organics of Fisher Scientific, U.S.A), Lauroglycol® 90 (Propylene glycol monolaurate, Gattefosse, France), Labrasol® (caprylocaproyl macrogol-8-glycerides, Gattefosse, France), Artemether (Hangzhou Dayang chemical, Hong kong China), high performance liquid chromatography (Waters 2487 Dual wavelength absorbance detector, Waters 717 plus Auto sampler, Waters 510 HPLC pump), Neusilin® FH2 (magnesium aluminum metasilicate, Fuji Chemicals Ind co ltd. Japan), Zeta Sizer (Malvern Instruments Ltd., UK), DV-111 ultra-programmable rheometer (Brookfield Engineering Labs, USA), seven station dissolution apparatus (Sotax services, USA), centrifuge (Mini Spineppendorf, U.S.A).

2.2 Methods

2.2.1 Calibration curve for artemether

A 1 mg quantity of artemether powder was dissolved in a mixture of 3.5 mL of acetonitrile and 1.5 mL of water (70:30). From this stock solution suitable sample volumes were diluted with similar solvent mixture to give the following concentrations: 20, 40, 80, 100, 150 and 200 µg/mL respectively. Samples were chromatographed by HPLC (Waters 2487 Dual wavelength absorbance detector, Waters 717 plus Auto sampler, Waters 510 HPLC pump) at 216 nm on a C18 matrix (4.6x100) at 1 mL/min using a mobile phase mixture of acetonitrile and water (70:30). Standard curves were determined using peak area integration.

2.2.2 Construction of pseudo-ternary phase diagram

Labrasol® (surfactant) and lauroglycol® 90 (co-surfactant) ratios were varied at fixed ratios of triacetin to generate 30 different anhydrous emulsion (AE) formulations (Table 1). Triacetin concentration was fixed at ratios 1,2,3,4 and 5 respectively. At each triacetin ratio while, the concentration of labrasol® was decreased that of lauroglycol® 90 was simultaneously increased, as shown in Table 1.

The titration method was adopted for the determination of self-emulsifying region. A 0.1 mL quantity of the AE was pipetted into a 10 mL beaker. Drop-wise quantities of Milli-Q water (Millipore, USA) filtered through a 0.22 µm filter was introduced into the beaker until a stable transparent system was formed. Formulations resulting in phase separation or cloudiness were discarded. The different amounts of the ingredients that contributed to transparent systems were determined and a phase diagram plotted using Sigma plot 11 (Sigma plot, USA).

Table 1. Batch composition (ratio of oil, surfactant and cosurfactant) for pseudoternary phase diagram construction

Batch #	Oil (Triacetin)	Surfactant (Labrasol)	Cosurfactant (Lauroglycol 90)
1	1	8	1
2	1	7	2
3	1	6	3
4	1	5	4
5	1	4	5
6	1	3	6
7	1	2	7
8	1	1	8
9	2	7	1
10	2	6	2
11	2	5	3
12	2	4	4
13	2	3	5
14	2	2	6
15	2	1	7
16	3	6	1
17	3	5	2
18	3	4	3
19	3	3	4
20	3	2	5
21	3	1	6
22	4	5	1
23	4	4	2
24	4	3	3
25	4	2	4
26	4	1	5
27	5	4	1
28	5	3	2
29	5	2	3
30	5	1	4

2.2.3 Solubility of artemether

An excess quantity of artemether was added to triacetin, labrasol® and lauroglycol 90® respectively, vortex-mixed for 15 min and filtered using a 0.1 µm syringe filter. A 20 µL quantity from each of the filtrates was diluted to 1 mL with acetonitrile and assayed for drug content using HPLC as described above.

2.2.4 Preparation of artemether-loaded anhydrous emulsion (AAE)

Drug-loaded anhydrous emulsion was prepared based on stable batches used for pseudo-ternary phase diagram construction. Artemether, 1.2 g, was added to a sufficient quantity of triacetin and vortexed. This was followed by the addition of labrasol® and lauroglycol® 90 and further mixed using a multipurpose rotator (Barnstead Lab-Line, Malaysia) to give a final concentration of 40 mg of artemether per 300 mg of formulation. The resultant AAE was

stored for further studies. Placebo AEs were prepared in a similar manner without the addition of artemether.

2.2.5 Thermodynamic studies: Effect of refrigeration/centrifugation

The AEs were subjected to a 12 hour cycle of refrigeration (4º C) and alternate storage at laboratory temperature condition of 25º C for one week. Thereafter observation was made for any evident phase separation or drug precipitation. In order to preclude the possibility of metastable conditions, the AEs were subjected to centrifugation (MiniSpin eppendorf, U.S.A) at 4500 rpm for 30 minutes and examined visually for phase separation and/or drug precipitation.

2.2.6 Droplet size, Polydispersity index and Zeta potential determinations

Transparent aqueous dispersions of AEs were prepared by gentle agitation of the AAEs with appropriate quantity of Milli-Q water. The droplet size, polydispersity index and zeta potential were determined using the Zeta Sizer (Malvern Instruments, U.K) at a light scattering angle of 90º.

2.2.7 Viscosity studies

Apparent viscosity was determined in duplicate using a DV-111 Rheometer (Brookfield Engineering Labs, USA) with a CPE 51 spindle and Rheocalc V3.1-2 software.

2.2.8 Loading efficiency of AAEs

Exactly 10 µL of AAE was diluted to 10 mL with acetonitrile, shaken to ensure complete dissolution and filtered through a 0.4 µm filter. The filtered solution was assayed for artemether content by HPLC as already described. All assays were done in triplicate.

2.2.9 Drug release studies

The dissolution apparatus (Sotax services, USA) was used. The dissolution chamber constituted of 7 glass bottles of about 100 mL volumes. Into each was introduced 100 mL of 0.1N HCl which was allowed to equilibrate to 37º C prior to the introduction of encapsulated AAE. Dissolution was run for 40 min at 3 min sampling time intervals. Samples were subsequently assayed for drug content using HPLC as already described.

2.2.10 Emulsification time

A 340 mg quantity of AAE was introduced into a beaker containing 200 mL of Milli-Q water at 37ºC and mounted on a hot plate prior to agitation using a magnetic stirrer. The rate of emulsification was monitored visually until cloudiness was constant.

2.2.11 Powderability and micromeritic evaluation of AAEs using magnesium aluminum metasilicate powder

The AAE was mixed with an equal volume of 95 % ethanol and added to a quantity of the powder to give an AAE to powder ratio of 3:4. The damp mass was blended using a glass rod, wet-screened through a no. 16 sieve (mean aperture size, 1.0 mm) and oven-dried at a temperature of 50º C for 30 min. The dry granulation was finally dry-screened through the

same sieve. Subsequently micromeritic evaluation of the AAE powder was carried out as described below.

2.2.12 Flow rate

A 19 g quantity of AAE powder was introduced into a glass funnel (orifice diameter 0.3 cm, efflux tube length 9.8 cm and surface diameter 10 cm) and the time to flow through the funnel was noted. The experiment was carried out in triplicate. The flow rate was calculated thus:

$$\boldsymbol{Flow\ Rate} = \frac{\boldsymbol{Weight\ of\ powder\ (g)}}{\boldsymbol{Flow\ time\ (s)}} \qquad \boldsymbol{Eq\ 1}$$

2.2.13 Bulk density

A 19 g quantity of the AAE powder was introduced into a measuring cylinder and the untapped volume noted. Triplicate determinations were made. The bulk density was calculated as:

$$\boldsymbol{Bulk\ Density} = \frac{\boldsymbol{Weight\ of\ powder\ (g)}}{\boldsymbol{Volume\ of\ powder\ (cm^3)}} \qquad \boldsymbol{Eq\ 2}$$

2.2.14 Tapped density

A 19 g quantity of the powder was introduced into a measuring cylinder and tapped to a constant volume. Tapped density was calculated as:

$$\boldsymbol{Tapped\ Density} = \frac{\boldsymbol{Weight\ of\ powder\ (g)}}{\boldsymbol{Volume\ of\ tapped\ powder\ (cm^3)}} \qquad \boldsymbol{Eq\ 3}$$

2.2.15 Derived properties

Some derived properties of the powders were also determined as follows:

$$\boldsymbol{Compressibility\ Index} = \frac{\boldsymbol{V_b - V_t}}{\boldsymbol{V_b}} \qquad \boldsymbol{Eq\ 4}$$

$$\boldsymbol{Hausner's\ Quotient} = \frac{\boldsymbol{V_b}}{\boldsymbol{V_t}} \qquad \boldsymbol{Eq\ 5}$$

Where V_b = bulk volume and V_t = tapped volume

2.2.16 Antimalaria studies

The authors declare that "principles of Laboratory Animal Care" (NIH publication no. 85-23, revised 1985) in accordance with the ethical standards laid down in the 1964 Declaration of Helsinki were followed. Experimental protocols were in compliance with and approved by the University of Nigeria, Nsukka animal ethics committee and compliant with the Federation of European Laboratory Animal Science Association and the European Community Council Directive. Mice used were obtained from the Faculty of Veterinary Medicine, University of Nigeria, Nsukka (UNN). Water and food were administered *ad libitum* at the Department of Pharmacology and Toxicology animal house (UNN). *Plasmodium berghei* parasites were obtained from the National Institute of Medical Research, Lagos, Nigeria. Peter's four-day

suppressive test was adopted [2]. A 0.2 mL quantity of donor mouse blood diluted with Phosphate buffer saline (PBS), containing parasitized erythrocytes was intraperitoneally inoculated into twenty five mice (parasetamia level, 9-12%) randomly divided into five groups of five mice per group. Treatment was initiated daily from day 0 through day 3 with 4 mg/kg of artemether administered orally. On the fourth day after establishing parasitemia, blood was collected from the mice and thinly smeared on a microscope slide. The blood films were fixed on the slide using methanol and stained with Giemsa, pH 1.2. The number of parasitized erythrocytes was recorded after counting 250 red blood cells from each slide. The mice from each group were also observed for day of death. Activity was calculated thus [26]:

$$Activity = 100 - \frac{mean\ parasitemia\ of\ treated\ group}{mean\ parasitemia\ of\ control}\ X\ 100 \qquad Eq\ 6$$

2.2.17 Statistics

All statistical calculations, optimization procedures, experimental design generation, and formulation projections were done with JMP version 4.0.4 software, SAS Institute Inc., Sigma plot 11 software and GraphPad Instat Demo. *P* values less than .05 were considered significant.

3. RESULTS AND DISCUSSION

3.1 Results

3.1.1 Solubility, Pseudo-ternary phase diagram, droplet size and polydispersity index

The solubilities of artemether in triacetin, labrasol® and lauroglycol® 90 were 81±5, 101±5 and 3.14±0.06 mg/mL respectively. Mixtures of triacetin, labrasol® and lauroglycol® 90 were prepared as AE according to the ratios summarized in Table 1. The water titration method was used to determine whether the potential AEs were self-emulsifying or not. Mixtures that exhibited phase separation or could not form transparent systems were discarded. On the other hand those mixtures that produced transparent systems were noted and a pseudo-ternary phase diagram plotted using (Sigma plot 11 software). Out of the 30 mixtures in Table 1 only batches 1, 2, 9 and 16 formed stable transparent emulsions in aqueous phase. The pseudo-ternary phase diagram shown in Fig. 1 identifies the self-emulsifying domain of potential AEs. As shown in Fig. 1, 50-70% of surfactant mix was required to effectively form stable transparent systems.

As shown in Table 2 the placebo formulations had significantly ($p<0.05$) lower droplet sizes than drug-loaded ones. Unfortunately, since the droplet size of batch 16 was over 1000 nm after drug loading it was not considered further. The aqueous dispersion of batch 1 recorded droplet size of less than 100 nm, typical of SMEDDS; while the >100 nm droplet sizes of batches 2 and 9 was characteristic of SEDDS. The polydispersity index which describes the degree of uniformity in droplet size was either about 0.1 or 0.2.

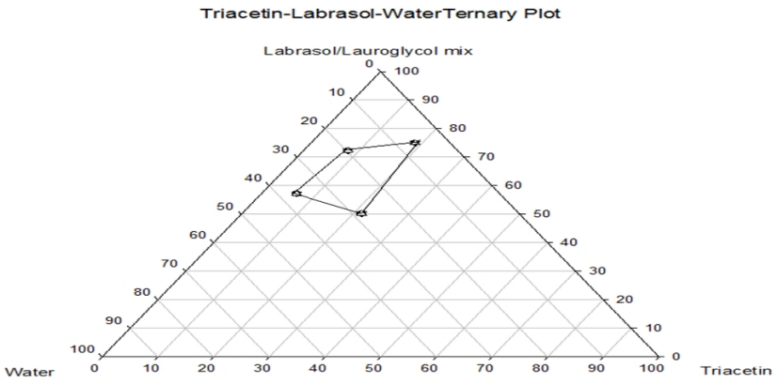

Fig. 1. Pseudoternary plot of labrasol/lauroglycol 90 mix, triacetin and water

Table 2. Droplet size and polydispersity index of aqueous dispersion of the placebo and artemether-loaded anhydrous emulsions.

Batch #	Placebo AEs		Artemether-loaded AEs	
	Droplet size (nm)	Poly dispersity index	Droplet size (nm)	Poly dispersity index
1	48.8±2	0.226±0.005	142±7	0.34±0.07
2	152±1	0.24±0.02	251±1	0.25±0.08
9	173± 14	0.14± 0.04	381±5	0.22±0.02

3.1.2 Factorial design

These batches (1, 2 and 9) produced emulsions with droplet sizes that were amenable to factorial design experiment. The purpose of this statistical design was to further optimize the different component proportions or independent process parameter values of the AE, using droplet size as the response, or evaluation index. Upon this premise a three-factor, two-level (2^3) design (with 3 middle-points) was chosen which resulted in 22 formulation options. Accordingly, 22 artemether-loaded AEs were prepared and assessed for thermodynamic stability (refrigeration and centrifugation) and viscosity; droplet size and polydispersity index of the aqueous dispersion were also evaluated, and the results shown in Table 3. Table 4 shows the Software-predicted AE compositions and properties while Table 5 shows the droplet sizes of the aqueous dispersions of statistically (software) predicted and experimental AAEs.

3.1.3 Effect of aqueous dilution on the optimized artemether-loaded anhydrous emulsions

The data in Table 6 show the effect of aqueous dilution on the droplet size, polydispersity index and zeta potential of the optimized formulations A, B and C. The droplet size and zeta potential values of 50 and 100-fold dilutions were significantly ($p<0.05$) higher than those of 2 and 3-fold dilutions. The PDI values of 100-fold dilution was <0.2 while other dilutions were >0.2.

Table 3. Factorial design for the preparation of artemether-loaded anhydrous emulsions, their properties and that of associated aqueous dispersions

Batch code	Factor level[1]	Oil (Triacetin)	Surfactant (Labrasol)	Cosurfactant (Lauroglycol 90)	Droplet size[3] (nm)	Poly dispersity index[3]	Refrigeration cycle[2]	Viscosity[2] (mPa s)	Stability on centrifugation[2]
F1	-+-	1	8	1	114±8	0.28±0.01	Stable	61±1	NP/PS[4]
F2	--+	1	7	2	232±3	0.166±0.001	Stable	52.3±0.4	NP/PS
F3	-++	1	8	2	95±2	0.291±0.004	Stable	58.1±0.3	NP/PS
F4	000	1.5	7.5	1.5	221±6	0.218±0.003	Stable	50.7±0.3	NP/PS
F5	000	1.5	7.5	1.5	218±9	0.24±0.03	Stable	49.9±0.1	NP/PS
F6	++-	2	8	1	251±23	0.23±0.08	Stable	53.8±0.3	NP/PS
F7	000	1.5	7.5	1.5	223±6	0.23±0.02	Stable	53.7±0.7	NP/PS
F8	--+	1	7	2	232±7	0.19±0.01	Stable	51±1	NP/PS
F9[5]	+-+	2	7	2	-	-	Stable	45.9±0.1	NP/PS
F10[5]	+-+	2	7	2	-	-	Stable	45.7±0.2	NP/PS
F11	-+-	1	8	1	118±6	0.274±0.001	Stable	53.3±0	NP/PS
F12	++-	2	8	1	250±7	0.24±0.07	Stable	55.1±0.2	NP/PS
F13	---	1	7	1	143±7	0.267±0.001	Stable	55.4±0.4	NP/PS
F14	000	1.5	7.5	1.5	230±7	0.21±0.02	Stable	50.7±0.1	NP/PS
F15	+--	2	7	1	366±12	0.16±0.05	Stable	50.9±0.2	NP/PS
F16	+--	2	7	1	356±8	0.19±0.08	Stable	49.9±0.1	NP/PS
F17	000	1.5	7.5	1.5	202±11	0.27±0.02	Stable	50.6±0.1	NP/PS
F18	---	1	7	1	138±3	0.26±0.02	Stable	55.2±0.1	NP/PS
F19	000	1.5	7.5	1.5	201±0.5	0.269±0.001	Stable	50.8±0.1	NP/PS
F20	+++	2	8	2	458±74	0.4±0.2	Stable	47.4±0.1	NP/PS
F21	-++	1	8	2	99±2	0.33±0.04	Stable	57.7±0.1	NP/PS
F22	+++	2	8	2	339±20	0.245±0.001	Stable	47.9±0.07	NP/PS

[1] - low level, 0 middle point, + high level
[2]Anhydrous emulsion (AE)
[3]Aqueous dispersion of the AE
[4]No drug precipitation or phase separation
[5]Could not form transparent system

Table 4. Software-predicted anhydrous emulsion compositions and properties

Batch code	Oil (Triacetin)	Surfactant (Labrasol)	Cosurfactant (Lauroglycol 90)	Droplet size	Desirability Index
1	1	7	1	138	0.168
2	1	7	1.25	155	0.208
3	1	7	1.5	173	0.249
4	1	7	1.75	190	0.290
5	1	7	2	207	0.331
6	1	7.25	1	120	0.125
7	1	7.25	1.25	137	0.166
8	1	7.25	1.5	155	0.207
9	1	7.25	1.75	172	0.247
10	1	7.25	2	189	0.288
11	1	7.5	1	102	0.082
12	1	7.5	1.25	119	0.123
13	1	7.5	1.5	136	0.164
14	1	7.5	1.75	154	0.205
15	1	7.5	2	171	0.246
16	1	7.75	1	84	0.044
17	1	7.75	1.25	101	0.081
18	1	7.75	1.5	118	0.122
19	1	7.75	1.75	136	0.163
20	1	7.75	2	153	0.203
21	**1**	**8**	**1**	**66**	**0.022**
22	**1**	**8**	**1.25**	**83**	**0.043**
23	**1**	**8**	**1.5**	**100**	**0.079**
24	1	8	1.75	118	0.120
25	1	8	2	135	0.161
26	1.25	7	1	191	0.292
27	1.25	7	1.25	208	0.333
28	1.25	7	1.5	225	0.374
29	1.25	7	1.75	243	0.416
30	1.25	7	2	260	0.459

Table 5. Droplet sizes of aqueous dispersions of software-predicted and experimental artemether-loaded anhydrous emulsions

Batch #	Oil (Triacetin)	Surfactant (Labrasol)	Cosurfactant (Lauroglycol 90)	Droplet size (nm)	
				Predicted	Experimental
A	1	8	1	65.0	68.4± 0.01
B	1	8	1.25	83.0	66.5± 4
C	1	8	1.5	100.0	70.6± 0.3

Table 6. Effect of aqueous dilution on the droplet size of experimental artemether-loaded anhydrous emulsions

Batch	2 fold dilution			3 fold dilution			50 fold dilution			100 fold dilution		
	DS[1] (nm)	PDI[2]	ZP[3] (-)	DS[1] (nm)	PDI[2]	ZP[3]	DS[1] (nm)	PDI[2]	ZP[3] (-)	DS[1] (nm)	PDI[2]	ZP[3] (-)
A	104.0±6	0.28± 0.01	0.5± 0.002	68.4± 0.01	0.25± 0.001	0.6±0 .03	377.0± 4	0.22±0 .04	6.0± 0.3	225.0± 16	0.10±0 .01	11.0±2
B	94.0±4	0.28± 0.01	0.4± 0.01	66.± 4	0.247± 0.002	0.5±0 .003	456.0± 3	0.34±0 .07	6.0±1	226.0± 6	0.12±0 .01	13.0±1
C	86.0±22	0.27± 0.03	0.5± 0.03	70.6± 0.3	0.25± 0.001	0.6± 0.01	326.0± 21	0.20±0 .01	6.1±0 .06	256.0± 8	0.17±0 .01	13.5±0 .6

[1] Dropet size (nm)
[2] Poly dispersity index
[3] Zeta potential

3.1.4 Drug release, emulsification time and loading efficiency

Drug release studies were carried out on the three experimental batches (A, B and C). The drug release reached 100 % within 3 min; so the release profile could not be obtained. The emulsification time values of batches A, B and C were as short as 3.12±0.31, 3.29±0.26 and 3.27±0.13 seconds respectively. The loading efficiency was between 95-100 % while the viscosity readings were between 58-62 mPa·s (as shown in Table 7). These batches had corresponding low droplet sizes. A similar observation was made earlier with respect to formulations (see Table 3) where viscosity values of 57, 58 and 60 mPa·s resulted in relatively low droplet sizes of 98, 95 and 114 nm respectively.

Table 7. Loading efficiency and viscosity values of artemether-loaded anhydrous emulsions

Batch code	Oil (Triacetin)	Surfactant (Labrasol)	Cosurfactant (Lauroglycol 90)	Viscosity (mPa s)	Loading efficiency, (%)
A	1	8	1	62±2	100
B	1	8	1.25	59±1	98
C	1	8	1.5	58.8±0.1	95

3.1.5 Micromeritic properties of the artemether-loaded anhydrous emulsions

The data in Table 8 show the various micromeritic properties of the AAE powder. According to Carr's classification [27] the angle of repose value and therefore flowability of batch C was fair while A and B rated as passable. Similarly batch C rated passable while, A and B had poor performance as per compressibility index and Hausner's quotient respectively.

Table 8. Some properties of artemether-loaded anhydrous emulsion powder

Batch code	AAE (mg)	MAM (mg)	FR (g/s)	AOR (°)	BD (g/cm^3)	TD (g/cm^3)	CI (%)	HQ
A	300	400	11.2±0.04	45±1°	0.58±0.01	0.85±0.03	32±2	1.46±0.03
B	300	400	9.7±0.2	41±2 °	0.67±0.02	0.90±0.05	26±2	1.35±0.04
C	300	400	10.1±0.7	39.6±0.8°	0.66±0.03	0.85±0.03	22±2	1.28±0.05

AAE (Artemether anhydrous emulsion); MAM (Magnesium aluminum metasilicate); FR (Flow rate); AOR (Angle of repose); BD (Bulk density); TD (Tapped density); CI (Carr's compressibility index); HQ (Hausner's quotient).

3.1.6 Antimalarial activity

Artemether AE showed antimalarial activity of 73.6 %; Artemether dissolved in ethanol solution, ie., ethanolic artemether (EA), 60.6%; Aqueous artemether (AA), 59.1 % and placebo AE, 20.2 % (Table 9). The % parasitemia values were subjected to analysis of variance (ANOVA) treatment. Results indicated that artemether-loaded anhydrous emulsion had significantly (P<0.05) lower % parasitemia than the rest of the formulations. In comparison to AAE the higher % parasitemia observed in the aqueous artemether-treated mice confirms superior antimalarial potential of the former. Furthermore there was no

significant (P<0.05) difference between the % parasitemia of ethanolic artemether-treated and aqueous artemether-treated mice. The AAE-treated mice' day of death (DOD) 22.0±2.6) was significantly (P<0.05) longer than that of EA (16±1.2), AA (14±1.6), placebo AE (10.4±1.1)-treated and untreated (10.4±2.1) mice respectively.

Table 9. % parasitemia and antimalarial activity results of the various sample batches

	AAE		EA		AA		Placebo		Untreated group	
BC	% PAS	DOD	% PAS	DOD	% PAS	DOD	% PAS	DOD	% PAS	DOD
1	11	20	18	15	15	12	34	9	40	8
2	12	19	13	16	14	14	28	10	38	12
3	09	22	12	18	19	16	35	11	41	13
4	10	25	17	16	18	15	30	12	39	10
5	09	24	16	15	13	13	27	10	35	9

Batch code (BC); AAE (Arthemether-loaded anhydrous emulsion-treated group); EA (Ethanolic arthemether solution-treated group); AA (Aqeous arthemether dispersion-treated group); Placebo (Placebo-treated group); % PAS (% Parasitemia); DOD (Day of death).

3.2 DISCUSSION

3.2.1 Pseudo-ternary phase diagram, droplet size and polydispersity index

The integral properties of the oil and surfactants largely determined the nature of the plot, as a change in each might introduce variation. The observed droplet size variation is attributed to the supplementary/synergistic effect of the oil and oily cosurfactant. Thus in Table 2, batch 1 consisting of 10 % each of oil and cosurfactant respectively resulted in a microemulsion (ME) with much lower (P<0.05) droplet size than batches 2 and 9 having 10 % oil, 20 % cosurfactant; and 20 % oil, 10 % cosurfactant respectively. Drug loading apparently inflated the droplet size considerably. The degree of diametric distension may be dependent on drug concentration, physicochemical properties of the drug in question and overall interaction in aqueous environment. The drug reservoir remains intact in the oil droplet, with the surfactant playing its interfacial role between the aqueous environment and the oil droplet. Droplet size plays a crucial role on *in vivo* behavior of SEFs in the gastro intestinal tract. Smaller droplet sizes are presented with higher interfacial area for drug absorption unlike larger ones [28, 29]. Besides, larger sizes may be predisposed to early drug precipitation prior to absorption. Polydispersity is the ratio of standard deviation to the mean droplet size 8 and is inversely proportional to droplet size uniformity; the higher the polydispersity the lower the uniformity of droplet size [7].

3.2.2 Thermodynamic studies

The stimulus for carrying out thermodynamic studies was to screen AEs for potential stability upon storage. All the 22 batches demonstrated stability (absence of phase separation or drug precipitation) during the 12 hour alternate refrigeration/laboratory temperature cycles. In addition, absence of drug precipitation or phase separation upon centrifugation further confirmed stability. Although AEs are reputed to possess thermodynamic stability, evaluation of their response to periodic alternate refrigeration and ambient temperature conditions is imperative to justify their stability. In tropical regions where oral liquid dosage forms require refrigeration after opening, it follows that stability under refrigeration and ambient temperature conditions be ascertained. In conventional emulsions where thermodynamic

stability is limited/absent phase separation of the internal phase is a huge threat during storage. Metastable AEs prepared with high drug-load may be prone to instability during storage or experimental centrifugation.

At 10 % oil and 80 % surfactant concentrations some formulations recorded comparatively higher (P<0.05) viscosities and lower droplet sizes than others. Thus, suggesting correlation between viscosity of AE and droplet size of the aqueous dispersion. Batches 9a and 10a (Table 3), could not form transparent systems, probably due to the high oil concentration constituted by triacetin and lauroglycol® 90.

3.2.3 Factorial design

The factorial design approach introduced middle points and other proportions. Phase diagram plots have been reported to incorporate hundreds of nanoemulsion formulations [30]. However they express component proportions in percent unlike factorial design which does not limit proportions to only percent as was typical of our experimental design (Table 2). As earlier stated all the software-generated 22 batches were experimentally translated into formulations and the droplet size and other parameters determined (Table 2). For the purpose of focus, droplet size the most crucial property of SEFs was utilized for optimization. Since the AEs were formulated with three component excipients (triacetin, labrasol® and lauroglycol® 90), it was necessary to determine which of the components impelled concentration-based significant variations in droplet size. Consequently the droplet size values of the 22 formulations were keyed into the appropriate column of the software Fit model command. The Fit model command graphically displayed the 'Whole model' and 'each model' effect, and details of ANOVA (analysis of variance). In addition an output grid Desirability table (Table 4) consisting of 125 different factor (constituent) levels (ratios) was generated. This is a compendium of different formulae and their corresponding predicted droplet sizes. The proportion ratios of the three factors differed by 0.25, characterized by more intermediate points different from the high, low and middle points as in Table 3.

Fig. 2 shows the Whole model plot of actual droplet size versus predicted values with a regression line and 95 % confidence curves. The regression line and the 95% confidence curves crossed the sample mean (horizontal line), an indication that the whole factorial model explains a significant proportion of the variation in droplet size [31]. The Leverage plots (not shown) for triacetin, labrasol® and lauroglycol® 90 also depicted that the regression line and the 95% confidence curves crossed the sample mean line, thus establishing that the three components (factors) significantly (P<0.05) contributed to and explained variations in droplet size. Contrarily, the Leverage plots for triacetin/lauroglycol® 90, triacetin/labrasol® and labrasol®/lauroglycol® 90 interactions respectively did not contribute significantly (P<0.05) to the droplet size variations since their regression lines and 95% confidence curves did not cross the mean line. Consequently, they were excluded from the Fit model interface, leaving only triacetin, labrasol® and lauroglycol® 90.

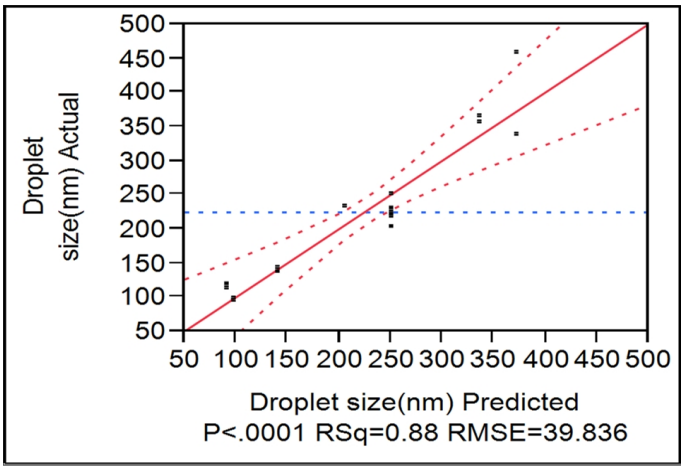

Fig. 2. First Whole model plot of Actual vs Predicted droplet size

The model was exclusively rerun with the above three factors, thus yielding a second Whole model plot (Fig. 3) and other leverage plots (Figs. 4-6). The regression line and 95% confidence curves of the Whole model plot still portrayed significance. However there was a little difference between this plot (Fig. 3) and the Whole model plot of Fig. 2. Fig. 2 incorporated non-statistically significant factor interactions while the second Whole model plot (Fig. 3) did not. As shown in Figs. 4-6 the three factors still indicated significance after rerun. The p value of triacetin (P<0.0001) was less than that of labrasol® (P=0.0069) and lauroglycol® 90 (P=0.0090) respectively which explains that variations in droplet size were mostly contributed by triacetin, followed by lauroglycol® 90 and lastly labrasol®.

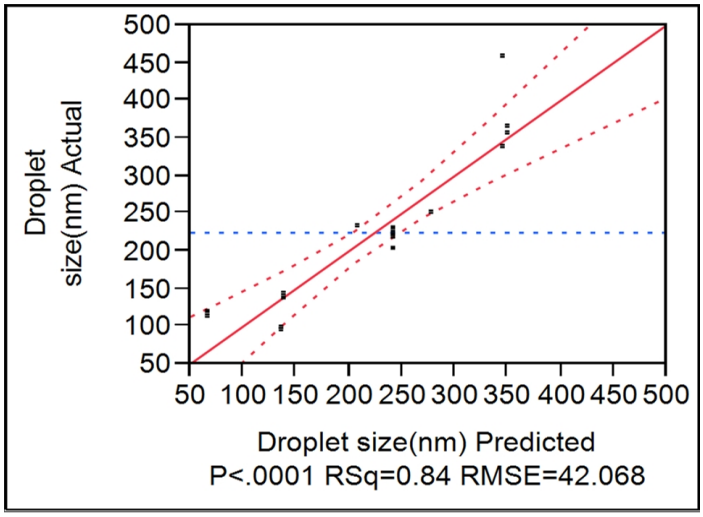

Fig. 3. Second Whole Model plot of Actual by Predicted droplet size (after elimination of Factor effects that were not significant)

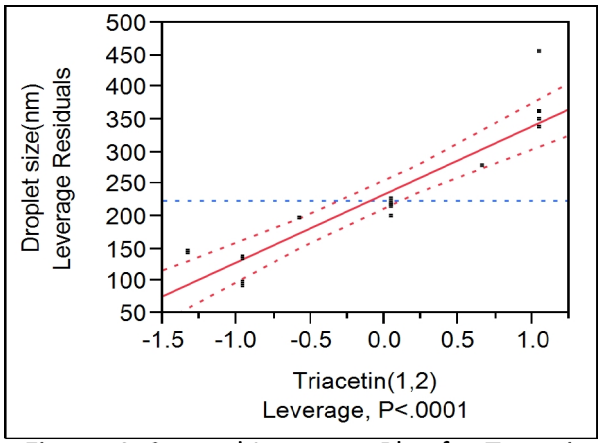

Fig. 4. Second Leverage Plot for triacetin

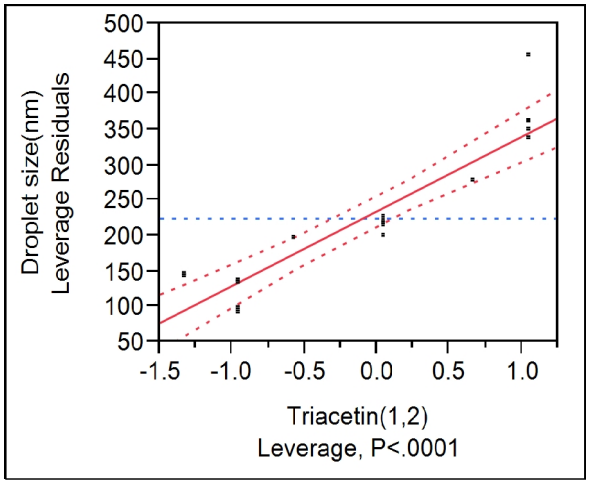

Fig. 5. Second Leverage plot for labrasol

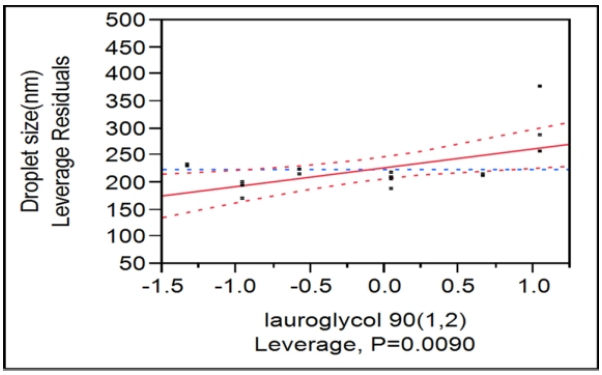

Fig. 6. Second Leverage Plot for lauroglycol 90

From the prediction profiler and Desirability plots (not shown) respectively . the maximum Desirability value was 0.874424, when triacetin and lauroglycol® 90 were at their highest settings (concentration ratios) of 2 and Labrasol® at its lowest setting (concentration ratio) of 7. Droplet size increased from 224.1615 nm at the centre of the factor ranges to 417.7076 nm at the most desirable setting. Desirability means the most desirable response value. In optimization the target is to discover factor (independent variable) levels (concentrations or settings) with optimal response. Typically, the prediction profiler reveals the best settings that produce the response target. In most cases response targets are required to be the highest values, hence the provision in the software for determining maximum desirability and the corresponding maximum response. This maximum desirability and the maximum droplet size was recorded by predicted batch no. 105 in Table 4 (the rest of the table was not included). However our goal was not for high droplet size values but the least. Hence, the choice of three batches (Table 5) with the least Desirabilites. Prior to maximization of desirability, the droplet size was 224.1615 nm at the highest triacetin setting (concentration ratio) of 2. On the other hand, its value at the lowest triacetin setting of 1 coupled with the lowest lauroglycol®90 setting of 1 and highest labrasol® setting of 8 was 95.03 nm. This was close to the predicted droplet sizes as contained in Table 5.

The factorial linear regression model equation is an algebraic representation of the regression line used for the description of the relationship between the response and predictor variables [19]. In our present investigation it is represented thus:

Response=constant + coefficient (predictor) +…
$Y=\beta_0+ \beta_1X_1+ \beta_2X_2+ \beta_3X_3+ \beta_4 X_1X_2+ \beta_5X_1X_3+\beta_6 X_2X_3$.

Where Y=droplet size, β=regression coefficient, X_1=triacetin, X_2=labrasol, X_3=lauroglycol® 90,
X_1X_2=triacetin/labrasol® interaction, X_1X_3=triacetin/lauroglycol® 90 interaction, X_2X_3 = labrasol®/lauroglycol® 90 interaction.

Since X_1X_2, X_1X_3 and X_2X_3 were excluded because of lack of significance, they were deleted from the equation, thus we now have, $Y=\beta_0+ \beta_1X_1+ \beta_2X_2+ \beta_3X_3$.

The coefficients from parameter estimates (Table not shown) were substituted appropriately in the equation to arrive at the model equation: $Y = 242+105X_1-36X_2+34X_3$.

Since optimization was our objective, batches 21-23 in Table 4 were selected as best (optimal) formulations, with values of 66, 83 and 100 nm and corresponding desirability values of 0.022, 0.043 and 0.079 respectively. Since these values were estimate predictions, we went ahead to experimentally formulate based on the software-suggested levels (ratios). The outcome would authenticate the dependability of the predictions. Post formulation droplet size results of the three batches represented as A, B and C are shown in Table 5. The result indicated a similarity between the predicted and formulated batches. The formulated batches recorded droplet sizes of less than 100 nm. This is suggestive that the factorial design experiment was capable of generating an empirically reproducible droplet size data for producing optimized formulations. This statistical approach proved robust, elaborate, powerful, reproducible and dependable; although time-consuming, in the long run the payload will be worth the effort for a pharmaceutical manufacturer who employs it in pre-formulation research.

3.2.4 Effect of aqueous dilution on the optimized AAEs

Orally administered SEF goes through a dilution process once in contact with gastric fluid. Our observation showed that droplet size changes would be dependent on volume of aqueous phase. SMEDDS are noted to resist drug precipitation for a longer time during gastrointestinal dilution and transit than SEDDS. The larger surface area of 100-fold dilution chiefly supported 'higher free mean path' (distance a droplet travels to witness collision) [32] that may have enhanced droplet motion, reduced droplet collision, diminished coalescence propensity and size enlargement. Ultimately, higher aqueous phase probably promoted more negative droplet zeta potential and low PDI (about 0.1). Droplets distances apart would embrace stable monodispersity [33]. Viscous AEs will probably result to higher emulsification times than less viscous ones. Generally all the batches produced did not indicate very high viscosity, hence the fast emulsification times recorded. Self-emulsification takes place when the entropy change favoring dispersion is more than the energy needed to increase the surface area of the dispersion [34-36].

3.2.5 Micromeritics

Generally batch C displayed the best micromeritic properties in comparison to the other two batches. It should be recalled that the AE formulations were adsorbed onto the base powder, magnesium aluminum metasilicate without the inclusion of popular flow aids (lubricant and/or antiadherent). This was a deliberate design to assess the potentiality of the powder to promote vehicular transformation of the liquid AE to powder in the absence of flow improvers. While the bulk density and flow rate values were relatively high, the compressibility index was high or poor amongst the batches. This is against the backdrop of some report that the density and flowability of powders are closely related, as dense particles generally possess better flow characteristics [37]. Conflicting flow indices are therefore not unusual. It has been argued that the simplistic sliding scale ranking of powders as either free-flowing or non-flowing is not substantive enough to address the problems that confront the equipment fabricator/designer and the pharmaceutical formulator. No one test or index could reliably reflect powder flowability [38]. During the tapped density experiment the usual consolidation of the granulations ensued. Generally for powders, tapped density is determined by tapping the powder mass until no further volume change or for a predetermined number of times. During this type of experiment powder/granule deformation does not often take place; but the contrary was the case with batches A, B and C respectively, due to the weakly aggregated particles in the granulations. Wet granulation is often associated with the formation of liquid bridges between particles, with the tensile strength of these bonds increasing as the quantity of granulating fluid increases. In the process of drying formation of interparticulate bonds due to the fusion or recrystallization and curing of the binding agent takes place [39-41]. Since the wet granulation employed in this work was with alcohol and excluded a binding agent the granules formed constituted particle agglomerates with very weak bonds. Consequently, upon tapping unusual consolidation and deformation probably gave rise to high tapped density values that resulted to high compressibility index.

The formulations in this work were preferentially intended for encapsulation in hard gelatin capsules. The result so far portends that encapsulation rather than tableting would be best suited for these powdered AAEs. The observed flow rate and bulk density would adequately suffice for reproducible uniform dose capsule filling. However in subsequent work attempt would be made to tablet the powder. Then, our investigation will ascertain the effect of consolidation and deformation within the die, as the lower and upper punch respectively,

perform their compaction tasks. In addition it is hoped that detailed characterization of the powder using DSC, SEM, TEM and FTIR shall be carried out. Until then suffice it to say that the powder excipient proved suitable for liquid solidification (powdering) of artemether AEs. While retaining fast emulsification time AAEs, when translated to powder posses the added advantage of preventing leakage of the AE.

3.2.6 Antimalarial studies

The improved aqueous solubility was a key-player to improved bioavailability and consequently antimalarial activity. Ontazolast loaded in SEDDS was reported to have improved bioavailability (compared to ontazolast suspension) probably via lymphatic absorption. It was explained that high drug concentration build-up may have occurred in the enterocytes through rapid absorption which occasioned improved lymphatic transport of ontazolast by a concentration-partitioning process [42,43]. This may explain the superior antimalarial activity of the AAE. Poor drug dissolution in the gastrointestinal tract (GIT) was probably responsible for the observed relatively low antimalarial activity of AA. Apart from poor water solubility artemether is known to be susceptible to the degradation effect of stomach acid [12]. SEDDS emulsify into nano droplets that offer gastro-protection to the entrapped drug solution and thus prevent contact between artemether and stomach acid. This may also have contributed to the observed highest antimalarial activity of the AAE.

For poorly soluble drug's aqueous solubility is critical to absorption. It is only the fraction of drug dissolved that is destined for absorption. The several current conventional oral forms of artemether in the market do not seem to address its poor water solubility. This may doom the intrinsic therapeutic efficacy of the drug through (future) possible drug resistance. Drug resistance may be possible in the face of erratic absorption and inherent short half life. It is arguable that the manufacturers leaflet instruction to coadminister with fatty meal smacks of ambiguity. For instance the amount of fat/oil is determined by the patient's dietetic habit which is affected largely by culture and health status. From the foregoing a lipid formulation of artemether may be more appropriate.

4. CONCLUSION

Artemether AE was formulated after a pseudo ternary phase diagram plot to delineate phase boundary. Subsequently a full factorial design approach was adopted to optimize the formulations. The three optimized AE formulations were translated to powder by adsorption onto magnesium aluminum metasilicate powder. Artemether AEs recorded higher droplet sizes than the placebo ones. The experimentally formulated batches indicated droplet sizes that ranked well with the predicted batches. Triacetin, the oil component of the formulation contributed most significantly ($P<0.05$) to droplet size variations. The fair and passable characteristics of some of the, artemether AE powders affirm their powderability. Artemether AE demonstrated highest antimalarial activity. In conclusion full factorial design has proved a reliable tool that optimized artemether self-emulsifying oil formulations with better antimalarial activity.

ETHICAL APPROVAL

The authors declare that "principles of Laboratory Animal Care" (NIH publication no. 85-23, revised 1985) in accordance with the ethical standards laid down in the 1964 Declaration of

Helsinki were followed. Experimental protocols were in compliance with and approved by the University of Nigeria, Nsukka animal ethics committee and compliant with the Federation of European Laboratory Animal Science Association and the European Community Council Directive.

ACKNOWLEDGEMENTS

We gratefully acknowledge the assistance of Dr. Roger Schnaare in review and revision of this manuscript. This work was funded by STEP B, University of Nigeria, Nsukka, Nigeria and arranged by Dr. Adeyeye to be carried out in Dr. Rohan's lab at the Magee Women's Research Institute at the University of Pittsburgh, PA. All the authors were involved in the conception, design and execution of the work. Neusilin® FH2 (Magnesium aluminum metasilicate) was a kind gift from Fuji Chemicals, USA, while labrasol® and lauroglycol® 90 were free samples from Gattefosse, USA.

DECLARATION OF INTEREST

There are no conflicts of interest among the authors.

REFERENCES

1. Hoar TP, Schulman JH. Transparent water-in-oil dispersions: the oleopathic hydro-micelle. Nature. 1943;152:102.
2. Schulman JH, Riley DP. X-ray investigation of the structure of transparent oil-water disperse system. I. J. Colloid Interface Sci. 1948;3:383.
3. Ashok RP, Pradeep RV. Preparation and in vivo evaluation of SMEDDS (self-microemulsifying drug delivery system) containing fenofibrate The AAPS. Journal. 2007;9(E3):44-52.
4. Fanun M. water solubilization in mixed nonionic surfactants microemulsions. Journal of Dispersion Science and Technology. 2008;29:1043-1052
5. Wei W, Yang W, Li Q. Enhanced bioavailability of silymarin by self microemulsifying drug delivery system. Euro J Pharm Biopharm. 2006;63(3):288–94.
6. CharmanWN, Stella VJ. Transport of lipophilic molecules by the intestinal lymphatic system. Adv Drug Deliv Rev. 1991;7:1–14.
7. Baboota S, Shakeel F, Ahuja A, Ali J, Shafiq S. Design, development and evaluation of novel nanoemulsion formulations for transdermal potential of celecoxib. Acta Pharm. 2007;57:315–32.
8. Dixit AR, Rajput SJ, Patel SG. Preparation and bioavailability assessment of SMEDDS containing valsartan. AAPS PharmSciTech. 2010; 11: 1.
9. Saraf S, Ghosh A, Kaur CD, Saraf S. Novel modified nanosystem based lymphatic targeting. Res J Nanosci Nanotech. 2011;1-15.
10. Trevaskis NL, Charman WN, Porter CJH. Lipid-based delivery systems and intestinal lymphatic drug transport: a mechanistic update. Adv Drug Deliv Rev. 2008;60:702-716.
11. Lefèvre G, Thomsen MS. Clinical pharmacokinetics of artemether and lumefantrine (riamet). Clin Drug Invest. 1999;18:467–480.
12. Joshi M, Pathak S, Sharma S, Patravale V. Solid microemulsion preconcentrate (NanOsorb) of artemether for effective treatment of malaria. Int J Pharm. 2008;362:172–178.

13. Sha X, Wu J, Chen Y, Fang X. Self-microemulsifying drug-delivery system for improved oral bioavailability of probucol: preparation and evaluation. Int Journ Nanomed. 2012;7:705-712.
14. Pouton CW, Porter JH. Formulation of lipid-based delivery systems for oral administration: Materials, methods and strategies. Adv Drug Deliv Rev. 2008;60:625–637.
15. Huang YB, Tsai YH, Yang WC, Chang JS, Wu PC. Optimization of sustained-release propranolol dosage form using factorial design and response surface methodology. Biol Pharm Bull. 2004;27:1626-1629.
16. Dobaria NB, Badhan AC, Mashru RC. A Novel Itraconazole Bioadhesive Film for vaginal delivery: design, optimization and physicodynamic characterization. AAPS PharmSciTech. 2009;10(3):951-959
17. Prakobvaitayakit M, Nimmannit U. Optimization of polylactic-co-glycolic acid nanoparticles containing itraconazole using 2(3) factorial design. AAPS PharmSciTech. 2003;4:E71.
18. Dhiman MK, Yedurkar PD, Sawant KK. Buccal bioadhesive system of 5-fluorouracil: Optimization and characterization. Drg Dev Ind Pharm. 2008;34:761–770.
19. Odeniyi MA, Jaiyeoba KT. Optimization of ascorbic acid tablet formulations containing hydrophilic polymers FARMACI. 2009;57(2):157-166.
20. Setthacheewakul S, Kedjinda W, Maneenuan D, Wiwattanapatapee R. Controlled release of oral tetrahydrocurcumin from a novel self-emulsifying floating drug delivery system (SEFDDS). AAPS PharmSciTech. 2011;12(1):152–164.
21. Tang J, Sun J, He Z. Self emulsifying drug delivery systems: Strategy for improving oral delivery of poorly soluble drugs. Curr Drg Ther. 2007;2:85-93.
22. Patil P, Joshi J, Paradkar P. Effect of formulatiuon variables on preparation and evaluation of gelled selfemulsifying drug delivery system (SEDDS) of ketoprofen. AAPS Pharm Sci Tech. 2004;5:34-42.
23. Aboelwafa AA, Makhlouf AIA. In vivo evaluation and application of central composite design in the optimization of amisulpride self-emulsifying drug delivery system. Amer Journ Drg Disc Dev. 2012;2(1):1-16.
24. Shaji J, Lodha S. Response surface methodology for the optimization of celecoxib self-microemulsifying drug delivery system. Ind J Pharm Scs. 2008;70(5):585-590.
25. Mahdi ES, Sakeena MH, Abdulkarim MF, Abdullah GZ, Sattar MA, Noor AM. Effect of surfactant and surfactant blends on pseudoternary phase diagram behavior of newly synthesized palm kernel oil esters. Drug Des Devel Ther. 2011;5:311–323.
26. Fidock DA, Rosenthal SL, Croft SL, Brun R, Nwaka S. Antimalarial drug discovery: efficacy models for compound screening. Nat Rev Drug Discov. 2004;3(6):509-520
27. Carr RL Jr. Classifying flow properties of solids. Chem Eng. 1965;1:69-74.
28. Gershanik T, Benita S. Self-dispersing lipid formulations for improving oral absorption of lipophilic drugs. Eur J Pharm Biopharm. 2000;50:179–88.
29. Gao P, Rush BD, Pfund WP, Huang T, Bauer JM, Morozowich W, et al. J Pharm Sci. 2003;92:2386-2398.
30. Shafiq-un-Nabi S, Shakeel F, Talegaonkar S, Ali ,J, Baboota S, Ahuja A, et al. Formulation development and optimization using nanoemulsion technique: A technical note. AAPS Pharm Sci Tech. 2007;2:28.
31. Cary NC. Introductory Guide, JMP® design of experiments, version 8. 2nd ed. SAS Institute Inc USA; 2009.
32. Wilkinson JB, Moore RJ. Emulsions. In: Wilkinson JB, Moore RJ, editors. Harry's cosmeticology. 7th ed. Essex, UK: Longman House, Burnt Mill, George Godwin publishers; 1982.

33. Patil P, Vandana P, Paradkar P. Formulation of self emulsifying drug delivery system for oral delivery of simvastatin: In vitro and in vivo evaluation. Acta Pharma. 2007;57:111-122.
34. Reiss H. Entropy-induced dispersion of bulk liquids. J Coll Interface Sci. 1975;53:61–70.
35. Bagwe RP, Kanicky JR, Palla BJ, Patanjali PK, Shah DO. Improved drug delivery using microemulsions: Rationale, recent progress and new horizons. Crit Rev Ther Drg Carrier Sys. 2001;118:77-140.
36. Moulik SP, Rakshit AK. Physicochemistry and applications of microemulsions. J surface Sci Technol. 2006;22:159-186.
37. Nada A, Al-Saidan SM, Mueller BW. Improving the physical and chemical Properties of ibuprofen. Pharm Tech. 2005;29: 11.
38. Prescott JK, Barnum RA. On powder flowability. Pharm Tech. 2000;60-84.
39. Banker GS, Anderson NR. Tablets. In: Lachman L, Lieberman HA, Kanig JL, editors. The theory and practice of industrial pharmacy. 3rd ed. Philadelphia: Lea and Febiger; 1986.
40. Gebre-Mariam TA. Nikolayev AS. Evaluation of starch obtained from Ensete ventricosum as a binder and disintegrant for compressed tablets. J Pharm Pharmacol. 1993;45:317-320.
41. Okafor SI, Chukwu A. The binding property of grewa gum II: Some physical properties of sodium salicylate tablets. W Afr J Bio Scs. 2003;14: 9-12.
42. Hauss DJ, Fogal SE, Ficorilli JV, Price CA, Roy T, Jayaraj AA, Keirns JJ. Lipidbased delivery systems for improving the bioavailability and lymphatic transport of a poorly water-soluble LTB4 inhibitor. J Pharm Sci. 1998;87:164–169.
43. Fricker G, Kromp T, Wendel A, Blume A, Zirkel J, Rebmann H, Setzer C, Quinkert R, Martin F, Müller-Goymann C. Phospholipids and lipid-based formulations in oral drug delivery. Pharm Res. 2010;27:1469-1486.

Peer-review history:
The peer review history for this paper can be accessed here:
http://www.sciencedomain.org/review-history.php?iid=280&id=14&aid=2164